# ChemComm

Accepted Manuscript


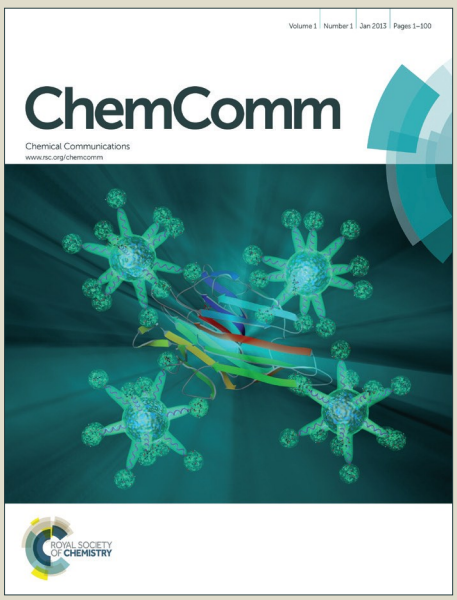





ROYAL SOCIETY OF CHEMISTRY

www.rsc.org/chemcomm

Journal Name

RSCPublishing

COMMUNICATION

# Combining a sensor and pH-gated Nanopore based on an Avidin-biotin system

APPROACHCite this: DOI: 10.1039/x0xx00000x

Mathilde Lepoitevin[a‡], Gael Nguyen[a‡], Mickael Bechelany[a], Emmanuel Balanzat[b], Jean-Marc Janot[a], Sebastien Balme[a]*

Received ooth January 2012,
Accepted ooth January 2012

DOI: 10.1039/x0xx00000x

www.rsc.org/

**Here we propose a new approach to tailor nanopores which combines both pH gated and sensor properties. This strategy is based on PEG like-avidin grafting in nanopores designed by atomic layer deposition (ALD). Below pH 5 the nanopore is blocked. We show that the PEG chains are at the origin of this property.**

Biological channels are involved in many tasks in biology such as cellular communication, osmotic pressure control and defence against external micro-organisms.[1] For the past two decades, biological channels[2] have served as an inspiration to building nanodevices such as ionic diodes[3] and sensors[4] which can precisely detect differences between ions,[5] small molecules or complex macromolecules such as DNA.[6] However the limitations of "raw" artificial nanopores are the lack of selectivity and unresponsiveness against biological stimuli such as pH, ionic strength, inhibitors or antibodies. However, this limitation can be broken by functionalization of nanopore.[7] Among artificial nanopores, the ones obtained by the track-etching methods on polymer films are particularly interesting. Indeed, their geometry can be controlled (cylindrical, conical)[8] and the chemical functions on the nanopore surface induced by the chemical etching process enable surface modification, such as functionalization by polymers[9] or DNA strands,[7b] or their size reduction by atomic layer deposition.[10] Several applications of these nanopores were demonstrated as ionic diodes,[3, 11] or voltage responsive nanopores.[12] More recently an elegant pH response nanopore by grafting DNA inside a conical nanopore was reported.[7b] In this paper authors used the isoelectric point of nucleotides to create a mesh which blocked current at low pH. However, these nanopore modifications were limited on a unique functionalization which is limited their applications to unique function. In order to build nanopores with different functions a strategy should be to use an avidin-biotin system.[13] Briefly, avidin is a glycoprotein which presents a strong interaction with biotin (Ka = 1015 M−1) which is a base for developing many kinds of biosensors.[13] This system allows us to build nanopores by multistep approaches after the functionalization of the nanopore surface with biotin.

Here we report the feasibility of a new type of nanopore which combines pH-gating and sensing properties. These single nanopores were obtained by using the track-etched method on PET film (13 µm). The first step consisted of grafting a PEG-biotin molecule to the surface of the nanopore following two approaches: (i) directly after chemically etching the nanopore and (ii) after reducing the diameter of the nanopore by atomic layer deposition (ALD) and the surface was functionalized by amine groups (Figure SI-1). Then, avidin (IP 10.6) or streptavidin (IP 5.6) were linked to the biotin. The obtained nanopores were tested for pH gating properties and detecting the presence of biotinylated γ-globulin.

The first approach of the nanopore modification was performed on both conical and cylindrical shaped nanopores. Cylindrical nanopores (~19 nm diameter) were directly functionalized after chemical etching. Since the surface of the nanopore is covered with carboxyl groups, the latter can be modified by chemical grafting. This involves using biotin with an amine end for a one-step N-(3-Dimethylaminopropyl)-N'-ethylcarbodiimide (EDC) modification process.[7b] In the first step, we attached poly(ethylene glycol) 2-aminoethyl ether biotin ($M_n$ 5300 g $mol^{-1}$) (Biotin-PEG-$NH_2$). The latter compound and EDC are placed in the cis reservoir of the electrochemical cell for 12 hours (Figure SI-1). Then, a solution of avidin (c= 2.44 µM, PBS 10 mM, NaCl 150 mM, pH 7.2) is placed in the cis reservoir for 30 min under a 100 mV voltage potential to help the protein enter the nanopore. After this step, the current-voltage dependence was recorded (Figure 1a) at different NaCl concentrations (Figure 1a and SI-2) and compared to the nanopore before functionalization. The avidin induces a weak decrease of current as expected due to a reduction of the nanopore diameter. The nanopore conductance is a function of the salt concentration (recorded at pH 7) allowing us to estimate the nanopore diameter (~17 nm) after avidin linkage (Figure 1b). Regarding intial diameter (~19 nm) the reduction of the nanopore diameter is ~2 nm. The latter value does not correspond to the hydrodynamic diameter of the avidin.[14] This is explained by a location of avidin close to nanopore entrance and not along nanopore lenght.[7c] We also observed after the avidin linkage current oscillations at high positive

voltage (typically from 800mV to 1V) regardless the salt used, KCl or NaCl (figure SI-2). The observation of such oscillations was reported in nanopores.[11b, 15] They result from different phenomena such as (i) vapor-gas equilibrium,[15-16] (ii) wetting dewetting,[11b] and (iii) the mobility of free polymer chains after chemical etching. However another explanation could be given. Indeed, proteins are well known to adsorb non-specifically at a liquid/solid interface.[17] It can be assumed that two populations of avidin are present in the nanopore, one linked to biotin and one adsorbed on the PET surface (particularly on the cis side, where PET is exposed to the protein). After rinsing, the adsorbed avidin can be released into the solution and translocate through the nanopore. This can also explain that oscillations are only observed when a positive voltage is applied on the trans chamber since avidin exhibits a negative charge at pH 7.

In order to estimate the localization of avidin inside nanopore and the non-specific adsorption on PET film, further investigations were performed by high resolution fluorescence confocal spectrometer.[17b] The latter technique allows measuring the fluorescence intensity through the thickness of the membrane by steps of 0.1 µm. For these experiments, we used avidin labeled by alexa-fluor 594 to allow its detection. Three different samples of PET film were used (i) a membrane with a nanopore previously functionalized by PEG-biotin (ii) one with a native nanopore and (iii) and one without nanopore. The spectra reported on SI-3 indicate the presence of avidin on PET surface due to nonspecific adsorption. We can also observe avidin inside the nanopore in both functionalized and native nanopore. However a higher fluorescence response located at the cis side of the membrane confirms a higher density of avidin where PEG-biotin is present. Regarding the non-specific adsorption, the previous assumption of avidin translocation, to interpret current oscillation should be taken into account.

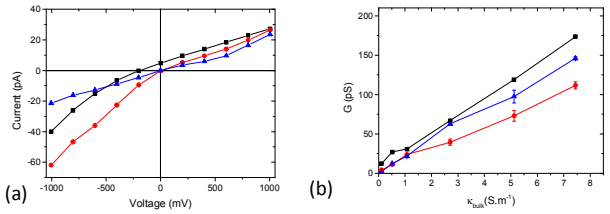


Figure 1. (a) Example of I-V curve (here under 100 mM NaCl pH 7) and (b) conductance/salt conductivity dependence of cylindrical nanopore at each step, directly after chemical etching (black), after PEG-avidin functionalization (blue) and after PEG-γ-globulin addition (red).

The first approach for nanopore modification was also performed on conical shaped nanopores (tip diameter 40 nm). In Figure 2 are reported examples of current-voltage dependence before and after avidin linkage. As previously described in the literature, I-V curves exhibit a current rectification.[18] After avidin linkage, the rectification is less important at negative voltage which proves the success of the functionalization. As previously mentioned the biotin-avidin allows considering multistep functionalization by addition of other biotinylated protein. We have tested if our nanopore (after PEG avidin functionalization) allows us to detect the γ-globulin modified by poly(ethylene glycol) (N-hydroxysuccinimide 5-pentanoate) ether 2-(biotinylamino)ethane (Biotin -PEG –NHS, Mn 5400 g mol$^{-1}$). To do this, the latter was added on the cis chamber of the electrochemical cell for one hour. We have chosen γ-globulin for its isoelectric point (6.5) close to neutral pH. In Figure 2a is reported an example of an I-V curve recorded at NaCl 100 mM pH 7. The PEG-γ-globulin induces a modification of current response under negative electric field. This proves the ability of this kind of nanopore to detect a biotin-PEG-protein. The I-V response under pH from 5 to 8 (figure 2b) is the most interesting part, since with the decrease of pH the current decrease.

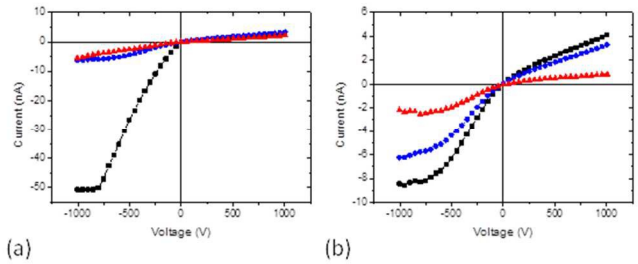


Figure 2. Conductance characterization of conical nanopore: (a) I-V curve (under 100 mM NaCl pH 7) conical nanopore at each step, directly after chemical etching (black), after PEG-avidin functionalization (blue), and after PEG-γ-globulin (red). (b) Influence of pH on nanopore conductivity after PEG-γ-globulin addition under 100mM NaCl pH 8 (black), pH 7(blue) and pH 5 (red)

From this first approach, we have shown the possibility to obtain both a pH dependence and sensing nanopore by successive functionalization. However, several points can be improved. First, we have shown a non-specific adsorption of avidin onto the nanopore surface. These adsorbed proteins should play a role since they could connect with biotin-PEG- γ-globulin and likely at the origin of the electrical oscillations. Then, the chemical conical etching allows predicting with difficulty the nanopore diameter.[19] Experimentally, if we want to tailor a nanopore with a precise diameter, several nanopores must be produced and individually characterized. Thus, this approach cannot be easily scaled up.

In order to break these limitations, we investigated a second approach. In order to control the diameter and be able to reproduce it easily, cylindrical nanopores were designed by atomic layer deposition. As previously reported this method allows us to control the size of the nanopore and to obtain a homogenous coating along the nanopore length.[20] We show here a typical result obtained with a nanopore with an initial diameter of ~48 nm determined by the nanopore conductance as a function of the salt concentration (SI-4). The nanopore was reduced by successive deposition of $Al_2O_3$/ZnO bilayers by ALD. The last layer (ZnO) enables the functionalization of free OH group when gaseous N-[3-(Trimethoxysilyl)propyl]ethylenediamine was added in order to graft amine groups on both, wall and external nanopore surface as confirmed by XPS characterization (SI -7). The final diameter of ~22 nm is obtained from the conductance as a function of the salt concentration. The second step consists of linking biotin-PEG at the amine end (Figure SI-1b). To do it a solution of poly(ethylene glycol) (N-hydroxysuccinimide 5-pentanoate) ether 2-(biotinylamino)ethane (Mn 5400 g mol$^{-1}$) is added on the cis reservoir of the electrochemical cell. After one hour, the nanopore is rinsed and a streptavidin (chosen for its IP ~5) solution is added in the same reservoir. Here both

external and internal surface of the nanopore are covered by PEG-biotin making unlikely the unspecific adsorption of streptavidin. After this step, the I-V curves are recorded at pH from 10 to 4 and NaCl 100 mM. At first, it can be noticed that the current traces recorded regardless the voltage do not exhibit oscillations. This should confirm our previous interpretation related to the translocation of released avidin in solution when nanopores were functionalized using the first approach.

The study of I-V response as a function of pH shows that for pH upper than 5 there is a weak current rectification as usually reported for conical nanopore. This current rectification is due to the dissymmetric nanopore functionalization.[7c, 21] Indeed, streptavidin have an isoelectric point close to 5, thus at pH ≥ 6 it exhibits a global negative charge. The localization of protein on cis side induces a difference of charge on nanopore surface wall. This induces an asymmetric flow of ion.[21] In addition, when a negative charge is applied on the trans side, the streptavidin are repelled from the nanopore, conversely than when a positive voltage is applied. In this case the current rectification could be also explained by the location of avidin (outside or inside the nanopore, regarding to the applied voltage and protein global) which could reduce the diameter of nanopore cis entrance. Interestingly, at pH values lower than 6 the current decreases dramatically. At pH 4 the nanopore is totally closed since the current is below -5 pA under -1V and 5 pA at 1V (Figure 3a and SI-5a). Our measurements show that the nanopore enclosure is reversible since after increase of pH buffer, the current values and the rectification are recovered. In addition, we have tested our nanopore under pH gradient (pH 4 in the cis chamber and 8 in the trans chamber). The current voltage dependence (Figure 3b) with a voltage range from -1V to 0.4 V shows that the current is close to zero and increases above voltages higher than 0.4 V. In addition, the current trace reveals a current gap at 0.35 V

This test confirms the pH dependence of the nanopore and the reversibility of the nanopore enclosure. The pH-gate observed at pH lower than 6 cannot be basically interpreted by a steric effect due to the avidin location inside or outside the nanopore cis entrance as previously mentioned. Indeed if this is the case one can expect an inversion of current rectification with the streptavidin global charge.

Thus, the nanopore enclosures at pH lower than 6 could become from PEG chain. In order to investigate this assumption, a similar nanopore functionalized with Biotinamidohexanoyl-6-aminohexanoic acid N-hydroxysuccinimide ester before streptavidin addition was tailored. The I-V curves at different pH do not exhibit a current blockage at pH 4 (SI-5b) which confirms that PEG is at the origin of current blockage.

It has been demonstrated that pH plays an important role on the PEG-protein interactions. This phenomenon is at the origin of protein aggregation and precipitation at low pH.[22] pH is also involved in swelling deswelling of PEG layer, on modified mesoporous material.[23] However, a nanopore (diameter ~10 nm) was functionalized with only PEG-biotin. In this case no pH influence on nanopore enclosure is observed. Thus pH below 6, the enclosure of our nanopore should be induced by protein-PEG interactions, likeky reversible aggregation. Under pH gradient and with respect to our experimental setup (SI-5a), when a negative voltage is applied, the protons enter preferentially inside the nanopore, thus the PEG-avidin aggregation encloses the nanopore. Conversely, when a positive voltage is applied, hydroxides enter the nanopore and induce a disaggregation of PEG-avidin and open the nanopore. The value of current gap 0.35 V should be interpreted by the local pH in cis entrance of nanopore and/or a dead time to reverse the enclosure mechanism.

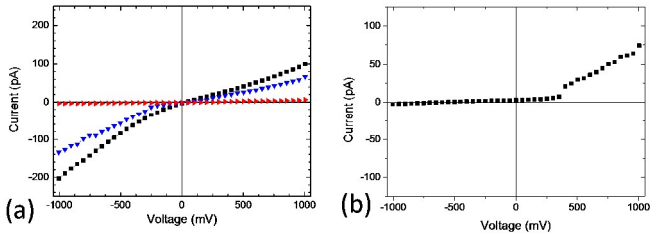


Figure 3. pH response of nanopore tailored by ALD after Biotin avidin functionalization (a) exemple of I-V curve after PEG-avidin grafting at pH 10 (black), pH 7 (blue) and pH 4 (red). (b) I-V curve under pH gradient (in black pH 4 in cis chamber and pH 8 in trans chamber)..

The potentiality to detect a biotinylated protein was evaluated by addition of biotin-PEG-γ-globulin. The latter is added on the cis reservoir (the same as streptavidin before). The current voltage curves (Figure 4a, SI-6) at different pH exhibit: (i) a current rectification at pH upper than 6 and (ii) a current blockage at pH lower than 6. Thus the pH-gate properties are not affected by biotin-PEG-γ-globulin addition. However at pH upper than 6, the current amplitude decreases weakly and the current rectification is more pronounced. To illustrate that, the rectification factor calculated from the ratio between conductances under positive over negative voltage is reported on Figure 4b at different pH. The results show that the biotin-PEG-γ-globulin addition induces an increase of the rectification factor. From this measurement, the biotinylated protein can be easily detected at pH upper than 7. Concerning the exact location of γ-globulins, these experiments cannot permit to conclude. Indeed the latter can be located either (i) at the external surface close to the nanopore entrance, (ii) at nanopore entrance or (iii) inside the nanopore. However the weak decrease of current and the steric volume occupied by the PEG-streptavidin suggest that the γ-globulins are outside the nanopore close to its entrance and unlikely inside the nanopore.

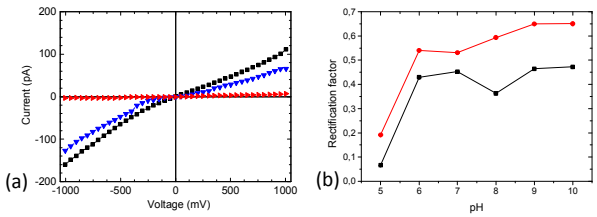


Figure 4. pH response of nanopore tailored by ALD after γ -globulin addition (a) example of I-V curve after PEG-streptavidin γ -globulin grafting at pH 10 (black), pH 7 (blue) and pH 4 (red). (b) Ratio between conductance under positive over negative, before (in black) and after (in red) γ-globulin addition

To sum up our results, we have shown two different approaches to biotinylated PET nanopores (i) directly after chemical etching and (ii) after nanopore modification using atomic layer deposition and surface functionalization by amine groups. After avidin linkage, the addition of PEG- γ globulin can be detected at pH higher than 7 using current-voltage measurements. Even if, in this paper we have not optimized

our nanopores, this result allows us to consider a large number of applications as a biosensor based on avidin-biotin system. The most fascinating part is the reversible nanopore enclosure observed at pH lower than 6 induced by the modification of the thickness of the PEG layer. In addition this phenomenon is totally reversible. This property opens applications such as membrane for drug delivery as suggested by Duan et *al.*[24] that ables to control both the rate and the location in the body of the drug release and in electrochemical (bio)sensors for the controlled gating of ions.[25] With further investigation, we hope that this new concept will enable to combine both pH gate and biosensor properties to achieve smart nanopore able to mimic biological channel.

## Notes and references

[a] Institut Européen des Membranes, UMR5635 ENSM UM2 CNRS, Place Eugène Bataillon, 34095 Montpellier cedex 5, France
[b] Centre de recherche sur les Ions, les Matériaux et la Photonique, UMR6252 CEA-CNRS-ENSICAEN, 6 Boulevard du Maréchal Juin, 14050 Caen Cedex 4, France
‡ These authors contributed equally to this work.
* Corresponding author sebastien.balme@univ-montp2.fr

Electronic Supplementary Information (ESI) available: [material and methods section, exemple of current trace, confocal fluorescence spectra, additional I-V curve and XPS]. See DOI: 10.1039/c000000x/

### Acknowlegments

This work was supported in part by the French Research Program ANR-BLANC, Project TRANSION (ANR-2012-BS08-0023) and by European Institute of Membrane by health project (PS2-2014). Single tracks have been produced in GANIL (Caen, France) in the framework of an EMIR project. We acknowledge Prof. A. Medhi (Université Montpellier 2) for enlightening discussions.

1. Domene, C.; Haider, S.; Sansom, M. S., *Curr Opin Drug Di De*, 2003, **6**, 611-619.
2. Siwy, Z. S.; Howorka, S., *Chem Soc Rev*, 2010, **39**, 1115-1132.
3. Vlassiouk, I.; Siwy, Z. S., *Nano Lett*, 2007, **7**, 552-556.
4. (a) Kowalczyk, S. W.; Blosser, T. R.; Dekker, C., *Trends Biotechnol*, 2011, **29**, 607-614; (b) Schneider, G. F.; Dekker, C., *Nat Biotechnol*, 2012, **30**, 326-328.
5. Balme, S.; Picaud, F.; Kraszewski, S.; Dejardin, P.; Janot, J. M.; Lepoitevin, M.; Capomanes, J.; Ramseyer, C.; Henn, F., *Nanoscale*, 2013, **5**, 3961-3968.
6. (a) Harrell, C. C.; Choi, Y.; Horne, L. P.; Baker, L. A.; Siwy, Z. S.; Martin, C. R., *Langmuir*, 2006, **22**, 10837-10843; (b) Chen, P.; Gu, J. J.; Brandin, E.; Kim, Y. R.; Wang, Q.; Branton, D., *Nano Lett*, 2004, **4**, 2293-2298; (c) Merchant, C. A.; Healy, K.; Wanunu, M.; Ray, V.; Peterman, N.; Bartel, J.; Fischbein, M. D.; Venta, K.; Luo, Z. T.; Johnson, A. T. C.; Drndic, M., *Nano Lett*, 2010, **10**, 2915-2921; (d) Storm, A. J.; Storm, C.; Chen, J. H.; Zandbergen, H.; Joanny, J. F.; Dekker, C., *Nano Lett*, 2005, **5**, 1193-1197; (e) Wanunu, M.; Sutin, J.; Meller, A., *Nano Lett*, 2009, **9**, 3498-3502.
7. (a) Li, Y. Q.; Zheng, Y. B.; Zare, R. N., *Acs Nano*, 2012, **6**, 993-997; (b) Buchsbaum, S. F.; Nguyen, G.; Howorka, S.; Siwy, Z. S., *J Am Chem Soc*, 2014, **136**, 9902-9905; (c) Nasir, S.; Ali, M.; Ramirez, P.; Gomez, V.; Oschmann, B.; Muench, F.; Tahir, M. N.; Zentel, R.; Mafe, S.; Ensinger, W., *Acs Appl Mater Inter*, 2014, **6**, 12486-12494.
8. Apel, P. Y., *Radiation Measurements*, 2001, **34**, 559–566.
9. Barsbay, M.; Guven, O.; Bessbousse, H.; Wade, T. L.; Beuneu, F.; Clochard, M. C., *J Membrane Sci*, 2013, **445**, 135-145.
10. Abou Chaaya, A.; Le Poitevin, M.; Cabello-Aguilar, S.; Balme, S.; Bechelany, M.; Kraszewski, S.; Picaud, F.; Cambedouzou, J.; Balanzat, E.; Janot, J. M.; Thami, T.; Miele, P.; Dejardin, P., *J Phys Chem C*, 2013, **117**, 15306-15315.
11. (a) Vlassiouk, I.; Smirnov, S.; Siwy, Z., *Nano Lett*, 2008, **8**, 1978-1985; (b) Pevarnik, M.; Healy, K.; Davenport, M.; Yen, J.; Siwy, Z. S., *Analyst*, 2012, **137**, 2944-2950.
12. Siwy, Z.; Heins, E.; Harrell, C. C.; Kohli, P.; Martin, C. R., *J Am Chem Soc*, 2004, **126**, 10850-10851.
13. Orth, R. N.; Clark, T. G.; Craighead, H. G., *Biomed Microdevices*, 2003, **5**, 29-34.
14. Balme, S.; Janot, J. M.; Dejardin, P.; Seta, P., *J Photoch Photobio A*, 2006, **184**, 204-211.
15. Shimizu, S.; Ellison, M.; Aziz, K.; Wang, Q. H.; Ulissi, Z.; Gunther, Z.; Bellisario, D.; Strano, M., *J Phys Chem C*, 2013, **117**, 9641-9651.
16. Buyukdagli, S.; Manghi, M.; Palmeri, J., *Phys Rev Lett*, 2010, **105**.
17. (a) Andrade, J. D.; Hlady, V., *Adv Polym Sci*, 1986, **79**, 1-63; (b) Balme, S.; Janot, J. M.; Dejardin, P.; Vasina, E. N.; Seta, P., *J Membrane Sci*, 2006, **284**, 198-204.
18. Schiedt, B.; Healy, K.; Morrison, A. P.; Neumann, R.; Siwy, Z., *Nucl Instrum Meth B*, 2005, **236**, 109-116.
19. Apel, P. Y.; Ramirez, P.; Blonskaya, I. V.; Orelovitch, O. L.; Sartowska, B. A., *Physical Chemistry Chemical Physics*, 2014, **16**, 15214-15223.
20. Cabello-Aguillar, S.; Abou-Chaaya, A.; Picaud, F.; Bechelany, M.; Pochat-Bohatier, C.; Yesylevskyy, S.; Kraszewski, S.; Bechelany, M.; Rossignol, F.; Balanzat, E.; Janot, J. M.; Miele, P.; Dejardin, P.; Balme, S., *Physical Chemistry Chemical Physics*, 2014, **16**, 17883-17892.
21. Ali, M.; Nasir, S.; Ensinger, W., *Chem Commun*, 2015, **51**, 3454--3457.
22. (a) Atha, D. H.; Ingham, K. C., *J Biol Chem*, 1981, **256**, 2108-2117; (b) Miekka, S. I.; Ingham, K. C., *Arch Biochem Biophys*, 1978, **191**, 525-536.
23. (a) Mouawia, R.; Mehdi, A.; Reye, C.; Corriu, R. J. P., *J Mater Chem*, 2008, **18**, 4193-4203; (b) Corriu, R. J. P.; Mehdi, A.; Reye, C.; Thieuleux, C., *Chem Commun*, 2003, 1564-1565.
24. Duan, R. X.; Xia, F.; Jiang, L., *Acs Nano*, 2013, **7**, 8344-8349.
25. de Groot, G. W.; Santonicola, M. G.; Sugihara, K.; Zambelli, T.; Reimhult, E.; Voros, J.; Vancso, G. J., *Acs Appl Mater Inter*, 2013, **5**, 1400-1407.



 